Theor Appl Climatol
DOI 10.1007/s00704-015-1715-4

ORIGINAL PAPER

Impact of Madden-Julian oscillation on onset of summer monsoon over India

R. Bhatla[1] · **Madhu Singh**[1] · **D. R. Pattanaik**[2]

Received: 22 October 2014 / Accepted: 20 December 2015

Abstract The Madden-Julian oscillation (MJO) is identified as the dominant mode of intraseasonal variabilities (ISVs) in the tropical atmosphere. It is one of the most influencing factors, which can influence the onset phase of monsoon over India giving rise to early/delayed onset of summer monsoon onset over Kerala (MOK) in the southern tip of India. The aim of the present study is to find years in which northward propagating ISVs significantly contribute to the early/delayed MOK. Climatology of early and delayed onset of Indian summer monsoon is analyzed in association with MJO state for the period of 37 years (1979–2015). The results indicate strong MJO events are frequent and show relatively better association with the onset of summer monsoon over India as compared to the weak MJO events. With respect to the MJO phase, the result suggests that the MOK occur mostly in association with MJO phases 1, 2, 3, and 8. Out of these, the MJO phase 2 (convection centre over western equatorial Indian Ocean) is mostly associated with pre-onset (early onset) years, MJO phase 8 (convection center over western hemisphere) is mostly associated with post-onset (late onset) years, and MJO phases 1 and 3 (convection centers over eastern equatorial Indian Ocean or western hemisphere) are mostly associated with normal-onset years.

✉ R. Bhatla
rbhatla@bhu.ac.in

[1] Department of Geophysics, Banaras Hindu University, Varanasi -221005, India

[2] India Meteorological Department, Lodi Road, New Delhi, India

1 Introduction

The southwest monsoon first arrives in the southeastern states of Kerala between late May and early June every year. Kerala is the gateway of summer monsoon to India. Southwest monsoon normally sets in over Kerala around 1 June. It advances northward, usually in surges, and covers the entire country around 15 July. Several studies have defined indices used to objectively derive the dates of monsoon onset over Kerala (Ananthakrishnan and Soman 1988; Fasullo and Webster 2003; Prasad and Hayashi 2005; Goswami and Xavier 2005; Joseph et al. 2006; Pai and Rajeevan 2009). Mohanty et al. (1982a, b) have investigated various parameters of heat and moisture budget during the First GARP Global Experiment (FGGE) for the period May–July 1979. Mohanty et al. (2005) analyzed the diagnostic aspects of the dynamics and energetics of the Asian summer monsoon and its spatial variability in terms of contrasting features of surplus and deficient summer monsoon seasons over India using reanalysis datasets. Raju et al. (2005) have categorized pre-onset, normal-onset, and post-onset period (each averaged 5 days) for the period 1948–1999 to investigate the mean circulation characteristics and the large-scale energetics of the Asian summer monsoon using the reanalysis datasets. Singh et al. (2007) have shown nonformation of onset vortex owing to highest warm pool SSTs and highest sea level pressure during Arabian Sea monsoon experiment (ARMEX) of 2003 monsoon season. Mao and Wu (2007) have proposed area-averaged meridional temperature gradient (200–500 hPa) as an index to define Bay of Bengal summer monsoon onset (BOBSM). Their study shows that the reversal of meridional temperature gradient (MTG) can capture the essential features of the BOBSM onset. Xavier and Goswami (2007) have developed an analog method to predict subseasonal variation of Indian summer monsoon (ISM) in advance up to four to five

Published online: 05 January 2016

pentads (20–25 days). Bhatla et al. (2015) examined the variations of surface meteorological fields and derived surface heat fluxes associated with onset of summer monsoon seasons over India based on 50-year data from 1957 to 2006.

The onset of summer monsoon over Kerala (MOK) represents significant transitions in the large-scale atmospheric and oceanic circulation in the Indo-Pacific region. Lau and Chan (1986) have shown that 40–50-day oscillation in the tropical convection is phase-locked to the monsoon onset over India. Their result suggests that eastward propagation is the basic property of equatorially trapped wave mode, and meridional propagation arises as a result of interaction between equatorial wave mode and monsoon circulation. The properties of MJO should be better described with each MJO episodes treated as a discrete pulse-like event propagating eastward with a phase speed of 5 ms^{-2} (Hendon and Salby 1994). Zhang (2005) has identified MJO as the dominant mode of intraseasonal (30–90 days) variability in the tropical atmosphere. Maharaj and Wheeler (2005) have used traditional method of time series analysis to predict daily bivariate index of MJO to describe convectively coupled, baroclinic structure of MJO along the equator. Love et al. (2008) has tested range of statistical models for their suitability in forecasting MJO signal. Wheeler and Hendon (2009) have shown impact of MJO on Australian rainfall and circulation during all four seasons, each composited contemporaneously for eight MJO phases derived from the real-time multivariate MJO index (Wheeler and Hendon 2004). MJO indices are measure of OLR anomaly, high value of OLR anomaly indicates cloud-free atmosphere, and low value of OLR anomaly indicates enhanced convection and cloud formation. MJO is said to have dipole nature with enhanced convection over Indian Ocean and a suppressed convection over Pacific Ocean and vice versa. Several studies have been carried out to find association between MJO phases and onset of the Indian summer monsoon (Wheeler and Hendon 2004; Pai et al. 2011). Barnes and Houze (2013) have shown deep convective entities in the central Indian Ocean and west Pacific Ocean associated with active MJO phases. Yaun and Houze (2013) have shown that greater frequency of occurrence of connected mesoscale convective systems (MCSs) coincide with increases in mid-tropospheric moisture observed in all convective regimes during large-scale convectively active MJO phases. Several hypotheses have been offered to explain how the initial convective onset of an MJO event occurs (Straub 2013; Adames and Wallace 2014). The present study aim to find years in which there is close association between northward propagating ISVs and onset of ISM. The outline of this study is as follows. The details of data and methodology have been given in Sect. 2. Section 3 is devoted to the discussion of the MJO state during MOK and changes in northward propagating convection anomaly from the equatorial Indian Ocean to the Indian subcontinent. Finally, the conclusions are given in Sect. 4.

2 Data and methodology

The dates of MOK were obtained from published material of IMD for the data period 1979–2015. The climatological mean date of MOK is 1 June, with a standard deviation of 6 days. Based on 37-year onset date of the ISM, we categorize the pre-onset, onset, and post-onset pentads (each an average of 5 days). The normal-onset years are those when the MOK is within ±2 days of its mean date of 1 June and is identified as P4 in Table 1. The pre-onset years are identified as P1 (third pentad prior to normal onset), P2 (second pentad prior to normal onset), and P3 (first pentad prior to normal onset), and the post-onset years are identified as P5 (first pentad after the normal onset) and P6 (second pentad after the normal onset) in Table 1. The real-time multivariate MJO indices (RMM1 and RMM2) of Wheeler and Hendon (2004) were used for defining strength and various phases of MJO. The data were obtained from (http://www.bom.gov.au/bmrc/clfor/cfstaff/matw/maproom/RMM/). The new RMM dataset is obtained from (http://www.bom.gov.au/climate/mjo/graphics/rmm.74toRealtime.txt) and (http://www.cpc.ncep.noaa.gov/products/precip/CWlink/MJO/mjo.shtml). The MJO is a tropical disturbance that propagate eastward around the global tropics with a cycle of 30–60 days. The convection anomaly associated with MJO propagate northward over Indian subcontinent. The MJO influences both the precipitation and surface temperature characteristics across the India. The Wheeler and Hendon (2004) suggested a two-dimensional phase-space diagram with RMM1 and RMM2 as the horizontal and vertical Cartesian axes respectively for viewing the evolution

Table 1 Pentad wise classification of onset period during 1979–2015

Pre-onset years		Normal-onset years		Post-onset years	
Year	Pentad	Year	Pentad	Year	Pentad
1985	P3	1980	P4	1979	P6
1988	P3	1981	P4	1983	P6
1990	P1	1982	P4	1986	P5
1993	P3	1984	P4	1992	P5
1994	P3	1987	P4	1995	P5
1999	P3	1989	P4	1997	P6
2001	P2	1991	P4	2003	P5
2002	P3	1996	P4	2005	P5
2004	P1	1998	P4	2012	P5
2006	P3	2000	P4	2014	P5
2007	P3	2008	P4	2015	P5
2009	P2	2010	P4		
2011	P3	2013	P4		
Total = 13		13		11	

P pentad

of the MJO. Phase and strength of MJO is determined using MJO indices.

MJO state can be computed using the following formula:

1. Amplitude (A) = $\sqrt{RMM1^2 + RMM2^2}$
2. Phase (θ) = $\tan^{-1}\frac{RMM2}{RMM1}$

The following criterion has been used to define strength of MJO:

1. Strong MJO event when $\sqrt{RMM1^2 + RMM2^2}.\geq 1$
2. Weak MJO event when $\sqrt{RMM1^2 + RMM2^2}. < 1$

The MJO phase-space diagram is divided into eight equal sectors representing eight phases of MJO evolution. Each of these phases represents approximate location of the MJO's convective envelope around the global tropics. MJO evolve in the Indian Ocean and propagate to Western Pacific through maritime continents. During MJO phases 1 and 2, formation of MJO associated with positive convective anomaly over the equatorial Indian Ocean. When the amplitude is greater than or equal to 1, these eight phases are categorized as "strong" MJO phases. When the amplitude is less than 1, irrespective of the phases of MJO, the MJO is categorized as "weak."

3 Results and discussion

Table 1 classify onset period (15 May to 13 June) into pre-, normal-, and post-onset years in terms of pentad (P1 stands for 15–19 May, P2 stands for 20–24 May, and so on with P6 stands for 9–13 June). It is clear from Table 1 that during 37 years of study period (1979–2015), 35 % events are pre-onset and normal-onset events while 30 % events are post-onset events. The result suggests that the probability of MOK to be a normal-onset year or a pre-onset year is large. There have been four such occasions (viz., 1980, 1982, 2000, and 2013) on which MOK occur on 1 June. MOK is earliest during years 1990 and 2004 (by three pentads), while MOK is most delayed (by two pentads) during years 1979, 1983, and 1997. There are 20 cases when MOK occur in the month of June and remaining 17 cases associated with MOK occur in the month of May.

Table 2 lists frequency of MJO phases with each phase having life cycle ≥6 days during onset period (P1 to P6) of MOK. There are maximum 7 (53 %) events out of 13 pre-onset events associated with MJO phase 2. The pre-onset years 1994, 2001, 2002, 2006, 2007, 2010, and 2013 are associated with MJO phase 2. However, maximum 6 (46 %) events out of 13 normal-onset events are associated with MJO phase 1 and phase 3. The normal-onset years 1980, 1987, 1991, 1996, 2008, and 2010 are associated with MJO phase 1, while normal-onset years 1984, 1996, 1998, 2000, 2008, and 2013 are associated with MJO phase 3. Thus, it is clear from Table 2 that pre-onset of monsoon is most favored by phase 2, while normal onset of monsoon is most favored by phase 1 and phase 3. The post-onset years show strong association with MJO phase 8. There are 10 (91 %) events out of 11 post-onset events associated with MJO phase 8. The post-onset events show 45 % association with MJO phase 1, phase 6, and phase 7.

Figure 1 gives daily range of MJO index amplitude for the onset pentads (P1–P6) during the period 1979–2015. The maximum MJO amplitude is seen in the year 1997 (a post-onset year), and minimum MJO amplitude is seen in the year 2014 (a post-onset year). The highest daily range of variation in MJO index amplitude is seen in the years 1998 (a normal-onset year) and 2004 (a pre-onset year), while lowest daily range of variation of MJO index amplitude is seen in the year 2007 (a pre-onset year). The interannual variability of mean MJO amplitude is shown in Fig. 2. The maximum mean MJO amplitude is seen in the year 1997 and minimum in the year 2014. It is clear from Fig. 2 that mean MJO amplitude increases during the period 1979–2015 (with the rate 0.002/year). The climatology of MJO amplitude for each MJO phase is shown in Fig. 3. It is found that MJO amplitude shows increasing trend (with the rate of 0.06/year). The MJO phase 7, phase 8, and phase 1 show the higher MJO amplitude during onset period (Fig. 3). Figure 4 shows the daily MJO amplitude variation (maximum–minimum) during different MJO phases. The highest day-to-day variation of MJO amplitude was seen during MJO phase 7. The day-to-day variation of MJO amplitude was higher during MJO phase 6 to phase 8.

Figure 5 shows frequency of the strong/weak MJO events for the period May 15 to June 13 during the period 1979–2015. Frequency of strong MJO events is more than the weak MJO events during all the eight phases of MJO. The strong MJO events are more frequent during MJO phases 3, 4, and 8 and less frequent during MJO phases 5, 6, and 7. During onset period, the MJO phases 4 and 8 are found to be more frequent as compared to MJO phases 1, 2, and 3. The MJO activity during onset period is found to be maximum during MJO phases 4 and 8 and minimum during MJO phases 6 and 7. The MJO phase 4 shows the maximum frequency during onset period, and MJO phase 6 shows the minimum frequency. The interannual variability of frequent MJO phases (life span ≥6 days) is shown in Fig. 6. The MJO phase 3 is the most frequent MJO phase (with 25-day life cycle) associated with onset of monsoon in the year 1984. The MJO phase 6 and phase 8 are the frequent MJO phases (with 21-day life cycle) associated with onset of monsoon in the year 1983.

The day-to-day variations of MJO amplitude during pre-onset, normal-onset, and post-onset years have been summarized in Fig. 7a–c. It is evident from Fig. 7a that the mean MJO amplitude is highest during the pre-onset year 2002 and least during the pre-onset year 2006. The highest daily range of MJO amplitude is seen in the year 2004, and the lowest range

Table 2 Frequency of MJO phases for the onset period during 1979–2015

MJO phase	Pre-onset years	Normal-onset years	Post-onset years	Frequency	Frequency of strong (weak) events (in days)
Phase 1	1994, 2006, 2007,	1980, 1987, 1991, 1996, 2008, 2010	1983, 2003, 2005, 2014, 2015	14 (38 %)	95 (45)
Phase 2	1994, 2001, 2002, 2006, 2007, 2010, 2013	1991, 1996	1979, 1995	11 (30 %)	98 (55)
Phase 3	1985, 1988, 1999	1984, 1996, 1998, 2000, 2008, 2013	1986	10 (27 %)	116(43)
Phase 4	1985, 1988, 1990,1994, 2004, 2011	1984, 1989, 2013	2012, 2014	11(29 %)	109(69)
Phase 5	1985, 1990, 2004, 2011	1989	2012	6 (16 %)	73(59)
Phase 6	1999 2009	1984,	1979, 1983, 1986, 2003, 2012	8 (22 %)	70 (52)
Phase 7	1982, 2009	1980	1992, 1997, 2003, 2005, 2015	8 (22 %)	88 (38)
Phase 8	1993, 2002, 2006, 2011	1982	1979, 1983, 1986, 1992, 1995, 1997, 2003, 2005, 2014, 2015	15 (41 %)	123 (50)

of daily MJO amplitude is seen in the year 2007. Figure 7b shows the day-to-day variation of MJO amplitude during normal-onset years. The highest range of daily MJO amplitude is seen in the year 1998, and lowest range of daily MJO amplitude is seen in the year 1980 (Fig. 7b). It is clear from Fig. 7b that during normal-onset year, the mean MJO amplitude is maximum in the year 1996 and mean MJO amplitude is minimum in the year 1989. The result shows higher variation of daily MJO amplitude during normal-onset years as compared to pre-onset years; however, the mean MJO amplitude is less during normal-onset years as compared to pre-onset years. Figure 7c shows the day-to-day variation of MJO amplitude during post-onset years. It is evident from Fig. 7c that mean MJO amplitude is highest during post-onset years as compared to normal- and pre-onset years; however, the daily range of MJO amplitude is minimal during post-onset years as compared to normal- and pre-onset years. The maximum mean MJO amplitude is seen in the post-onset year 1997, and minimum mean MJO amplitude is seen in the post-onset year 2014 (Fig. 7c). Analysis of the mean MJO amplitude and daily range of MJO amplitude suggests that the variation of MJO amplitude is highest during post-onset years although day-to-day variability is least during post-onset years. The day-to-day variability of MJO amplitude is highest during normal-onset years. One conclusion that can be drawn here is that there is increase in MJO strength during normal MOK, and there is decline in MJO strength during post-MOK.

Spatial distribution of monthly outgoing long-wave radiation (OLR) anomaly (W/m^2) during May and June is shown in Fig. 8a–c. The regions having negative (positive) OLR anomaly represents above (below) normal convection. OLR anomaly was within ±5 W/m^2 over the most parts of the country and adjoining seas (Fig. 8a). However, over some parts of west peninsula and adjoining Arabian Sea, negative OLR anomaly exceeds 10 W/m^{-2}. Over the equatorial Indian Ocean region, positive OLR anomaly exceeding 10 W/m^{-2} was observed. Pre-onset years are most favored by MJO phase 2 (Table 2), which is a region of enhanced convection (Fig. 8a). It may be one of the reasons responsible for enhanced convection (negative OLR anomalies) over north Arabian Sea, Bay of Bengal, and northeastern parts of the country during pre-onset period. Another region of enhanced convection is observed over maritime continents associated with MJO phase 4. A strong dipolar convective pattern associated with MJO phase 2 is evident from Fig. 8a. The noteworthy feature of pre-onset years is that

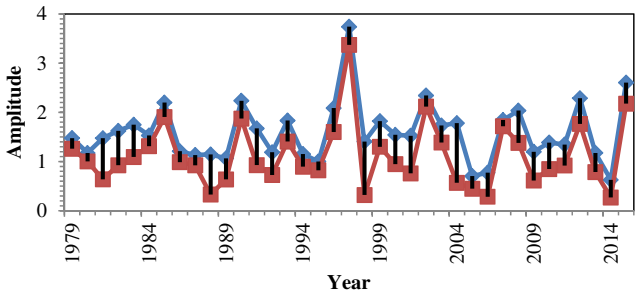

Fig. 1 Day-to-day variation of MJO amplitude (maximum–minimum), corresponding to onset pentads (P1 to P6) during the period 1979–2015

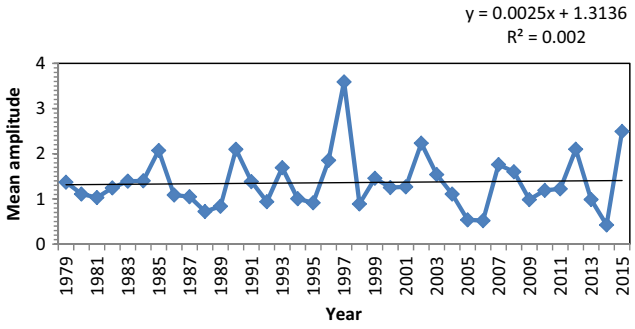

Fig. 2 Interannual variability of mean MJO amplitude corresponding to onset pentads during the period 1979–2015

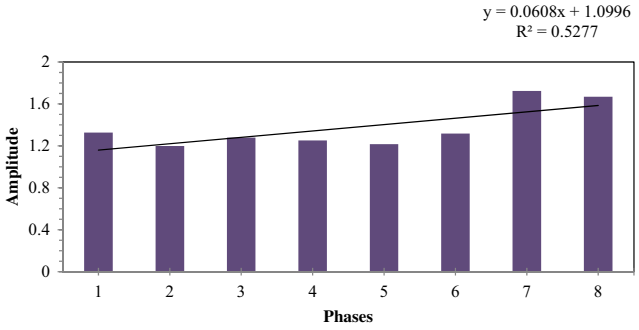

Fig. 3 Climatology of MJO phase1 to phase 8 amplitude for the onset period (May15 to June15) during the data period 1979–2015

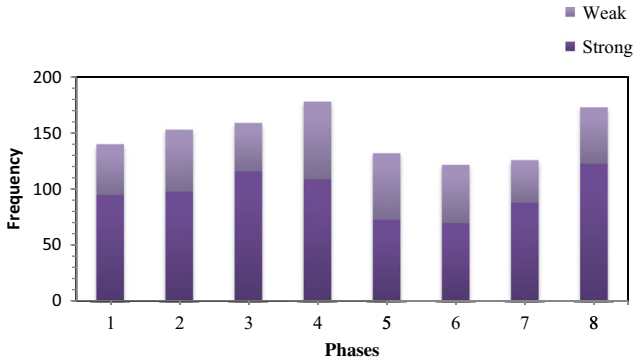

Fig. 5 Frequency (in days) of strong/weak MJO events corresponding to different MJO phases for the onset period during 1979–2015

it is associated with early MJO convective onset. It can be seen from Fig. 8b that OLR anomaly is less during normal-onset years (Fig. 8b) as compared to the pre-onset years. However, a weak dipolar convective pattern associated with MJO phase 1 and phase 3 prevailed during normal-onset years, and a strong dipolar convective pattern associated with MJO phase 2 prevailed during pre-onset years. Figure 8b suggests negative OLR anomaly over western Arabian Sea and equatorial Indian Ocean during normal-onset years is associated with MJO phase 1 and phase 3. It is evident from Fig. 8c that positive OLR anomaly over Central India, peninsular India, and Bay of Bengal is associated with negative OLR anomaly over MJO phase 1 region. Another region of positive OLR anomaly is associated with MJO phase 4. However, post-onset years are most favored during MJO phase 8 (Table 2) associated with enhanced convection over phase 8 region (Fig. 8c). An anomalous OLR pattern over Indian subcontinent and adjoining seas during post-onset years (Fig. 8c) explain the cause of delayed onset of ISM. The dipolar convective pattern is seen over phase 8 region. OLR anomaly during post-onset years is greater as compared to that during normal- and pre-onset years. The 850-hPa wind anomaly between 10° N–40° N and 40° E–100° E for pre-, normal-, and post-onset years is shown in Fig. 9a–c. The mean wind speed during pre-, normal-, and post-onset years is found to be 20, 15, and 10 ms^{-1}, respectively. A noteworthy feature of the 850-hPa wind vector anomaly is the westerly anomalies over Arabian Sea, south peninsular India, and Bay of Bengal and easterly anomalies over equatorial Indian Ocean associated with MJO phase 2. Wind analyses show strength of cross-equatorial flow over Arabian Sea in the month of May is stronger as compared to that over Bay of Bengal (Fig. 9a). Wind speed exceeds over Arabian Sea by 15–20 kts as compared to that over Bay of Bengal. Figure 9a suggests south-easterly wind at 10° S, and after crossing equator, it become south-westerly at around 5° N latitudes. There is a strong westerly wind anomaly over Arabian Sea as compared to that over Bay of Bengal. Strong low-level jet is evident from Fig. 9a which may be one of the possible causes of early MOK. However, there are low-strength winds over central India. Strong westerly anomalies over Arabian Sea (Fig. 9) associated with MJO phase 2 are supportive of positive convective anomalies over Arabian Sea (Fig. 9a). However, westerly wind anomalies associated with MJO phase 1 and phase 3 are less in the case of normal-onset years (Fig. 9b) which indicates small difference in the surface winds from the climatological mean winds. Strong easterly anomalies (Fig. 9a) over equatorial Indian Ocean are replaced by weak westerly anomalies during normal-onset years. It is evident from Fig. 9c that there is cyclonic circulation over southeastern parts of Arabian Sea during post-onset years (associated with MJO phase 8). Strong easterly anomalies are seen during post-onset years associated with MJO phase 2. Anomalous wind pattern during post-onset years (Fig. 9c) is supportive of anomalous convective pattern (Fig. 9c) in the equatorial Indian Ocean associated with MJO phase 8 during the post-onset years.

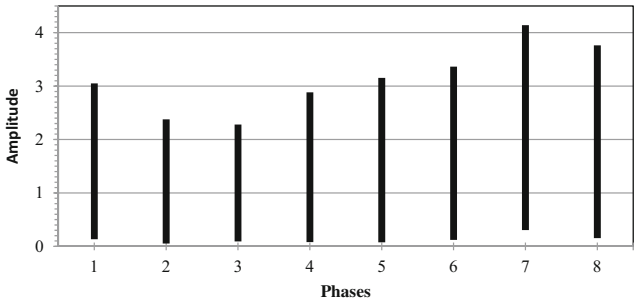

Fig. 4 Daily range of MJO phase 1 to phase 8 amplitude variation for whole onset period during the data period 1979–2015

The 200-hPa wind anomaly between 10° N–40° N and 40° E–100° E for pre-, normal-, and post-onset years is shown in Fig. 10a–c. The mean wind speed for pre-, normal-, and post-onset years is found to be 55, 40, and 50 ms^{-1}, respectively. A noteworthy feature of the 200-hPa wind anomaly is the formation of anticyclone over Pakistan and adjoining northwest India during pre-onset years (associated with MJO phase 2) and easterly to north-easterly flow (Fig. 10a). Winds are stronger over Indian landmass as compared to that over the Ocean.

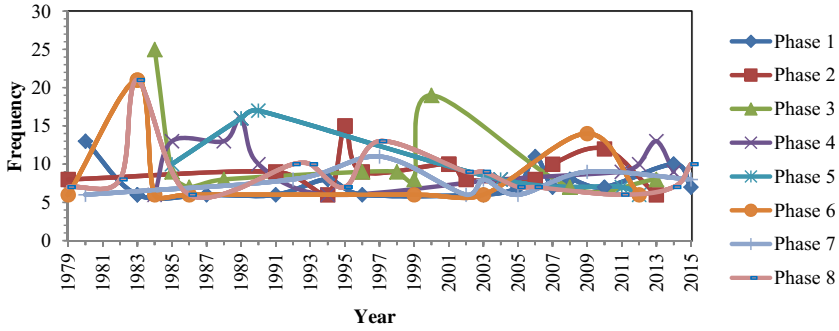

Fig. 6 Frequency of MJO phases 1 to 8 (≥6 days) during onset period for the data period 1979–2015

Wind anomaly analyses show strength of upper-level easterlies decreases in the case of normal-onset years (Fig. 10b). Anomalous wind pattern is seen during post-onset years (Fig. 10c) which may be one of the possible causes of the delayed onset of ISM. Wind anomaly analyses show westerlies (associated with MJO phase 8) instead of easterlies in the case of post-onset years (Fig. 10c). Composite results suggest that delayed MOK follows anomalous wind and OLR pattern over Indian subcontinent and adjoining Indian seas. However, OLR and wind anomaly is less in the case of normal-onset years (associated with MJO phase 1 and phase 3). It indicates small variation in OLR and wind anomalies from the climatological mean value. During onset southeastern states of Kerala and adjoining Arabian Sea is highly convective. The strength of northward propagating ISVs is responsible for early/delayed monsoon onset over India by transferring moisture and momentum from the deep tropics to the Indian subcontinent. The occurrence of enhanced (suppressed) rainfall during onset phase appears to result from induced upward (downward) motion within remotely forced lows (highs), and from anomalous low-level westerly (easterlies) winds that transport moisture from the tropics. Powell and Houze (2013) have proposed rapid increase in tropospheric humidity at 850 hPa over 3–7 days near MJO convective onset. Zhou and Murtugudde (2014) have shown contribution of the strong intraseasonal variabilities (ISVs) to the early onset of Indian summer monsoon (ISM) for the period 1982–2008. The years with significant contribution from ISVs are 1985, 1988, 1989, 1990, 2001, and 2004, which are referred to as ISVO years. Several studied have been carried out to know the association between MJO state and dates of monsoon onset over Kerala (Wheeler and Hendon 2004; Pai et al. 2011; Zhou and Murtugudde 2014). Many studies have suggested that the MJO acts to modulate the diurnal cycle (Chen and Houze 1997; Rauniyar and Walsh 2011; Oh et al. 2012; Peatman et al. 2014).

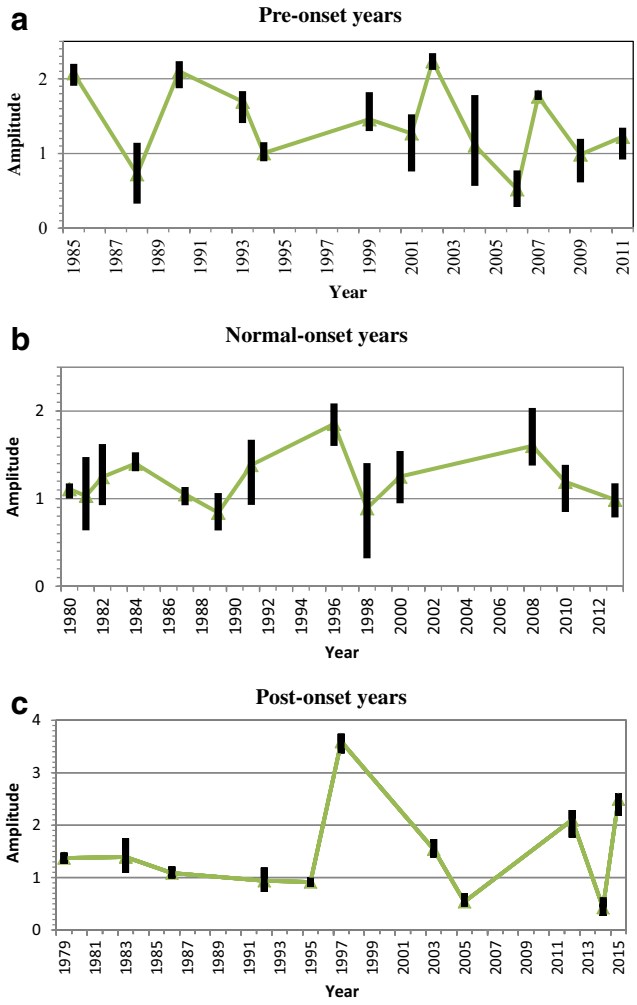

Fig. 7 Day-to-day variation of MJO amplitude/mean amplitude for the a pre-onset, b normal-onset, and c post-onset years during the period1979–2015

The results of the present study are consistent with the previous results that strong (weak) northward propagating ISVs significantly contribute to the early (delayed) onset of ISM. Dipolar convective pattern associated with MJO activity were seen over Indian Ocean and Indian subcontinent. The negative OLR anomalies during pre-onset years suggest above normal convection and rainfall (associated with MJO phase 2 region). During pre-onset years, strong cross-equatorial flow and cyclonic circulation supportive of positive convective anomalies is seen over Indian subcontinent and is associated with early MJO convective onset.

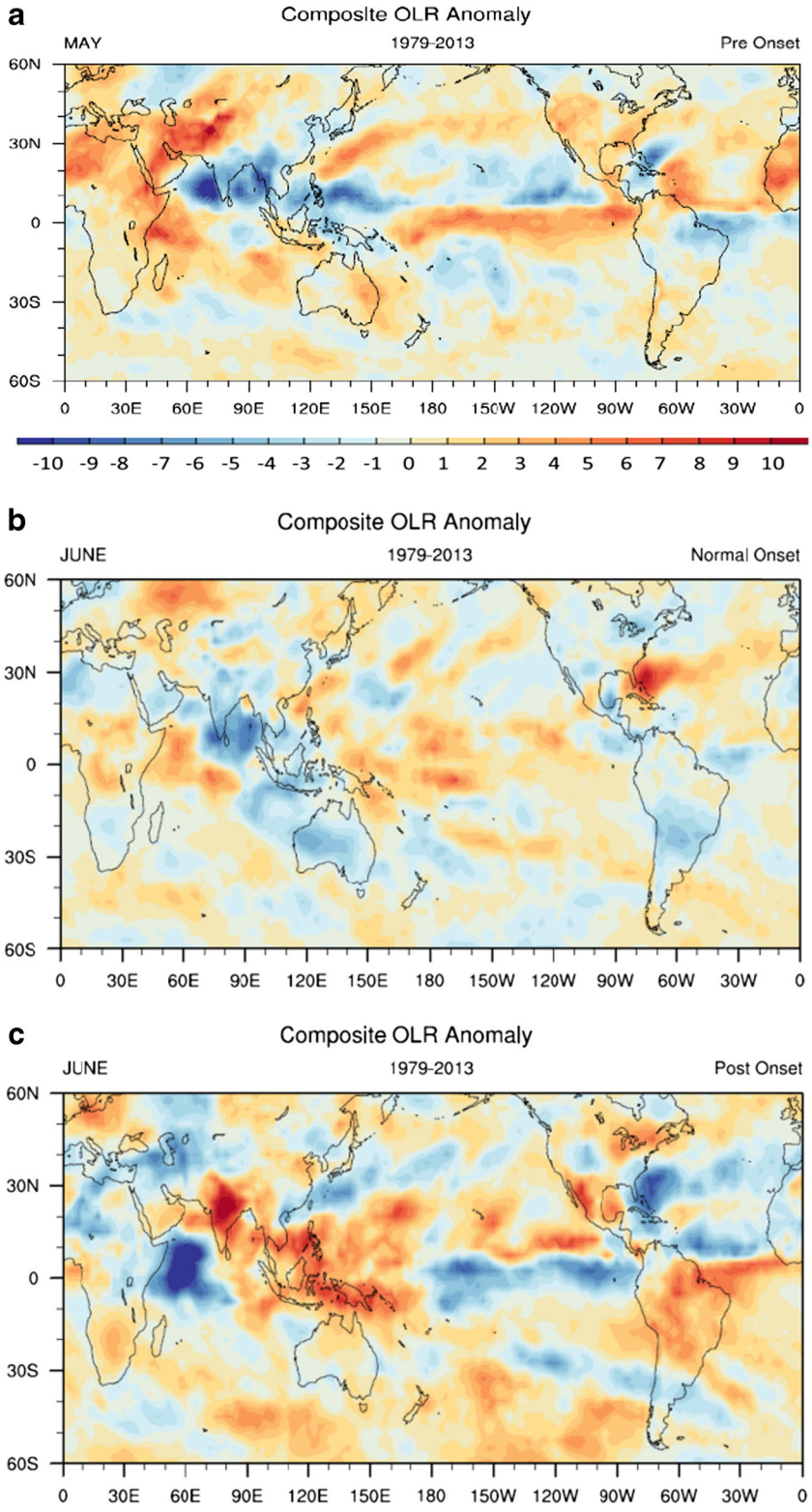

Fig. 8 Composite OLR anomaly (W m^{-2}) for the a pre-onset, b normal-onset, and c post-onset years during the period 1979–2013

The positive OLR anomalies during post-onset years suggests below normal convection and rainfall (associated with phase 8). The post-onset years are associated with suppressed convection in the Indian Ocean associated and enhanced convection in MJO phase 8 regions. The monthly wind anomalies at 850 and 200 hPa gives the indirect influence of MJO tropical convective anomalies on early/delayed set up of the monsoon which may result in the enhanced (suppressed) rainfall activity during onset period.

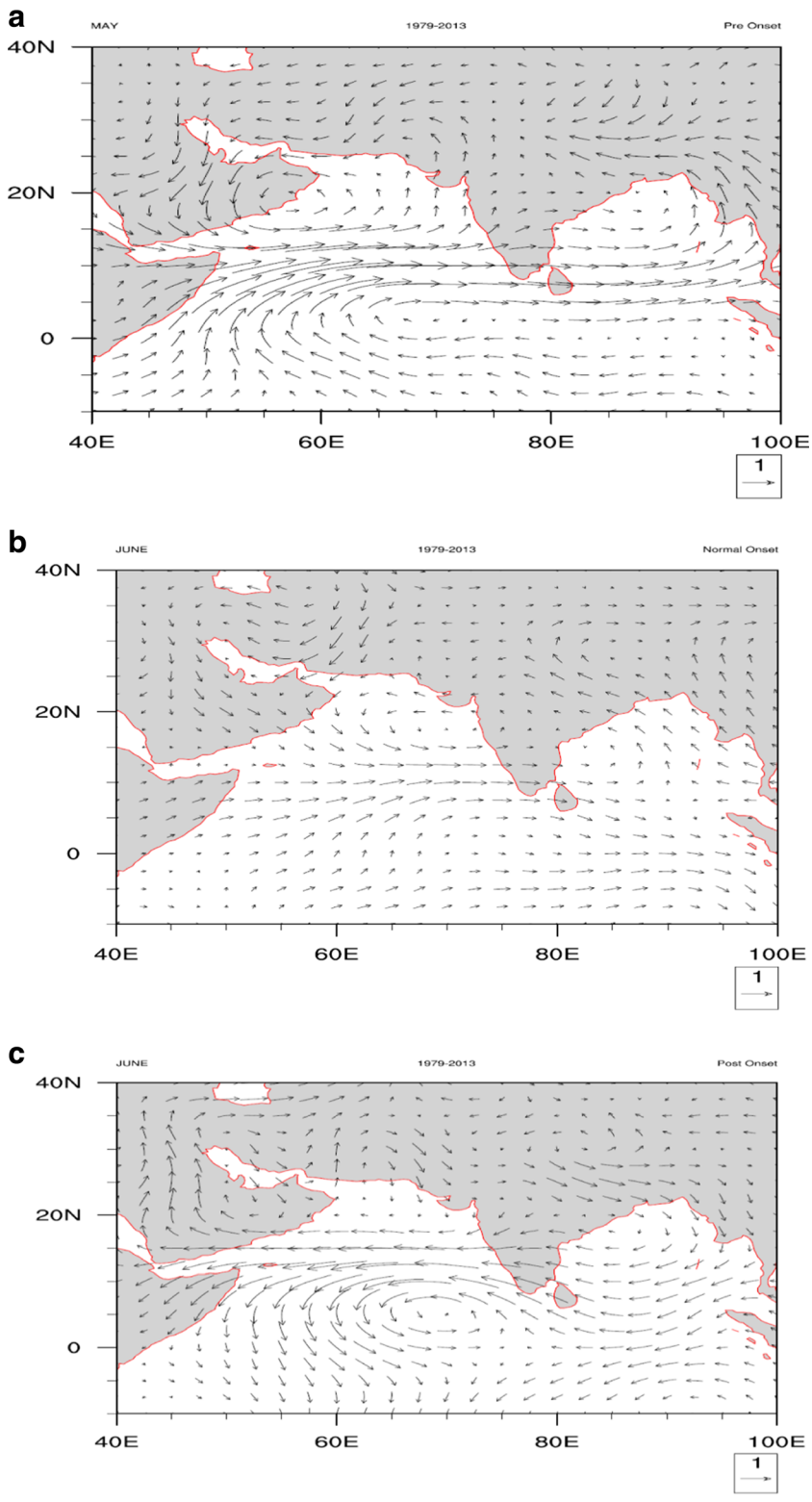

Fig. 9 Wind anomaly (ms^{-1}) at 850 hPa for the a pre-onset, b normal-onset, and c post-onset years of MOK during the period 1979–2013

4 Conclusion

The presents study provides MJO-MOK association during the period 1979–2015. The MJO modulates the diurnal cycle during the onset period (May 15 to June 13). The core region of MJO is located at low latitudes (between the equator and 15°) in the summer hemisphere, and it interacts with the monsoon circulation prevailing during the onset period. Thus, it may enhance (suppress) the onset process. The strong MJO events are relatively better associated with the onset process.

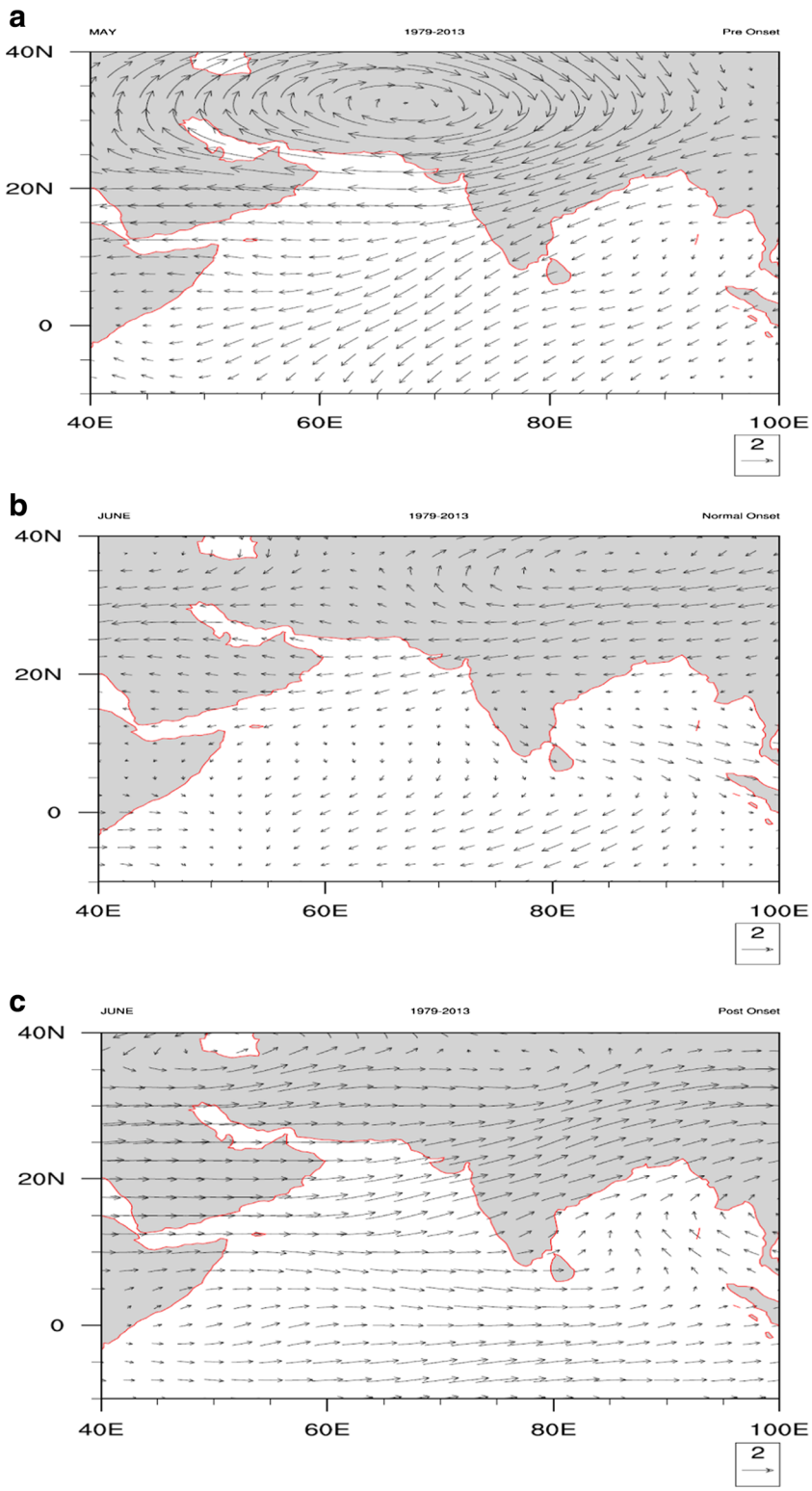

Fig. 10 Wind anomaly (ms^{-1}) at 200 hPa for the a pre-onset, b normal-onset, and c post-onset years of MOK during the period 1979–2013

During the period 1979–2015, MOK events are accompanied by 65 % strong MJO events and remaining 35 % MOK events are accompanied by weak MJO events. The onset of summer monsoon is associated with strong MJO phases 1, 2, and 4. However, strong MJO activity was mostly seen during MJO phase 2 (72 % cases) and phase 8 (71 % cases). The MJO phase 4 and phase 8 are the most frequent phases during onset period. The day-to-day variation of MJO-amplitude was highest during MJO phase 7 and phase 8. The MJO phase 1 (37 % cases) and phase 8 (40 % cases) are found to be longer

sustained phases with life cycle greater than 6 days (mean life cycle of each phase). During the period 1979–2015, phase 3 shows the longest sustained period of 25 days in the year 1984 which is comparable to MJO half cycle. The MJO phase 6 and phase 8 has sustained for 21 days in the year 1983 during onset period. The mean MJO amplitude averaged over onset period was highest in the year 1997. The climatology of MJO phase 1 to phase 8 mean amplitude suggests that mean amplitude of MJO phases has increased during the period 1979–2015 (with the rate 0.06/year). However, the MJO mean amplitude averaged over onset pentads shows less increase (with the rate 0.002/year). The day-to-day variation of MJO amplitude averaged over onset pentads was highest during normal-onset years, and the day-to-day variation of MJO amplitude was least during post-onset years. Pre-onset years show better association with MJO phase 2 which indicate early MJO convective onset during early MOK. However, normal-onset years show better association with MJO phase 1 and phase 3 and post-onset years show strong association with MJO phase 8. Before onset of ISM, convective features are prominent over Arabian Sea and Bay of Bengal. The dipolar convective pattern was strong during pre-onset years (convection centre over phase 2 region) and dipolar convective pattern was weak during post-onset year (convection center over MJO phase 8 region). The above (below) normal convection and rainfall was seen during pre (post) onset years. The MJO convective onset in the equatorial Indian Ocean enhances the onset process by modulating the diurnal cycle during onset period. The MJO is often quite variable with period of moderate to strong activity followed by period of little or no activity and reversal of phases during onset period. MOK occur during enhanced convective phases of MJO. Thus, MJO enhances the onset process which results in above normal convection and rainfall. The present study provides better insight on role of MJO in modulating monsoon current during onset of ISM. The results of this study may be helpful in forecasting the MJO convective onset in the equatorial Indian Ocean during onset period. This analysis indicates that the early/delayed onset of ISM depends on the timing of intraseasonal oscillation in the Indian Ocean and propagation of convective episodes into the western Pacific.

Acknowledgments The onset dates used in this study was obtained from the India Meteorological Department publication, which is thankfully acknowledged. The authors thank the Bureau of Meteorology Research Centre-Australia for availability of RMM data of MJO.

References

Ananthakrishnan R, Soman MK (1988) The onset of southwest monsoon over Kerala: 1901–1980. Int J Climatol 8:283–296

Adames A, Wallace JM (2014) Three-dimensional structure and evolution of the MJO and its relation to the mean flow. J Atmos Sci in press

Barnes HC, Houze Jr RA (2013) The precipitating cloud population of the Madden-Julian oscillation over the Indian and west Pacific Oceans. J Geophys Res 118:6996–7023

Bhatla R, Raju PVS, Mall RK and Bist Sanjay (2015) Study of surface fluxes during onset of summer monsoon over India. Int J Climatol DOI: 10.1002/joc.4462

Chen SS, Houze RA (1997) Diurnal varation and life-cycle of deep convective systems over tropical Pacific warm pool. QJR Meteorol Soc 123:357–388

Fasullo J, Webster PJ (2003) Hydrological definition of Indian monsoon onset and withdrawal. J Clim 16:3200–3211

Goswami BN, Xavier PK (2005) ENSO control on the south Asian monsoon trough the length of the rainy season. Geophy Res Lett 32: L18717. doi:10.1029/2005GL023216

Hendon HH, Salby ML (1994) The life cycle of the Madden-Julian Oscillation. J Atmos Sci 51:2225–2237

Joseph PV, Sooraj KP, Rajan CK (2006) The summer monsoon onset process over south Asia and an objective method for the date of monsoon onset over Kerala. Int J Climatol 26:1871–1893. doi:10.1002/joc.1304

Lau KM, Chan PH (1986) Aspects of the 40–50 day oscillation during the Northern Summer as inferred from outgoing long wave radiation. Mon Wea Rev 114:1354–1367

Love BS, Mattews AJ, Janacek GJ (2008) Real-time extraction of the Madden-Julian Oscillation using empirical mode decomposition and statistical forecasting with a VARMA model. J Clim 21:5318–5335

Mao J, Wu G (2007) Interannual variability in the onset of the summer monsoon over the eastern bay of Bengal. Theorol Appl Climatol 89: 155–170

Maharaj EA, Wheeler MC (2005) Forecasting an index of the Madden-Julian oscillation. Int J Climatol 25:1611–1618

Mohanty UC, Dube SK, Sinha PK (1982a) On the role of large scale energetic in the onset and maintenance of summer monsoon-I: heat budget. Mausam 33(2):139–152

Mohanty UC, Dube SK, Sinha PK (1982b) On the role of large scale energetic in the onset and maintenance of summer monsoon-II: moisture budget. Mausam 33(3):285–294

Mohanty UC, Raju PVS, Bhatla R (2005) A study on climatological features of the Asian summer monsoon: dynamics, energetics and variability. Pageoph 162:1511–1541

Oh JH, Kim KY, Lim GH (2012) Impact of MJO on the diurnal cycle of rainfall over the western maritime continent in the austral summer. Clim Dyn 38:1167–1180

Pai DS, Bhate J, Sreeejith A (2011) Impact of MJO on the intraseasonal variation of summer monsoon rainfall over India. Clim Dyn 36:41–55

Pai DS, Rajeevan MN (2009) Summer monsoon onset over Kerala: new definition and prediction. J Earth Syst Sci 118(2):1–13

Peatman SC, Matthews AJ, Stevens DP (2014) Propagation of the Madden–Julian Oscillation through the Maritime Continent and scale interaction with the diurnal cycle of precipitation. Q J R Meteorol Soc 140(680):814–825

Prasad VS, Hayashi T (2005) Onset and withdrawal of Indian summer monsoon. Geophys Res Lett 32:L20715. doi:10.1029/2005GL023269

Powell SW, Houze RA (2013) The cloud population and onset of the Madden-Julian Oscillation over the Indian Ocean during DYNAMO-AMIE. Jl Geoph Res Atmos 118(21):11–979

Raju PV, Mohanty UC, Bhatla R (2005) Onset characteristics of the southwest monsoon over India. Int Jl Clim 25:167–182

Rauniyar SP, Walsh KJE (2011) Scale interaction of the diurnal cycle of rainfall over the Maritime Continent and Australia: influence of the MJO. J Clim 24:325–348

Singh OP, Hatwar HR, Onkari P (2007) Surface and upper air meteorological features during onset phase of 2003 monsoon. J Earth Syst Sci 116(4):305–310

Straub KH (2013) MJO initiation in the real-time multivariate MJO index. J Clim 26:1130–1151

Wheeler MC, Hendon HH (2004) An all-season real-time multivariate MJO index: development of an index for monitoring and prediction. Mon Wea Rev 132:1917–1932

Wheeler MC, Hendon HH, Cleland S, Meike H, Donald A (2009) Impacts of the Madden-Julian oscillation on the Australian rainfall and circulation. J Clim 22:1482–1498

Xavier PK, Goswami BN (2007) An analog method for real-time forecasting of summer monsoon sub-seasonal variability. Mon Wea Rev 135:4149–4160

Yaun J, Houze Jr RA (2013) Deep convective systems observed by a-train in the tropical Indo-Pacific region affected by the MJO. J Atmos Sci 70:465–486

Zhang C (2005) Madden-Julian oscillation. Rev Geophys 43:1–36

Zhou L, Murtugudde R (2014) Impact of northward- propagating intraseasonal variability on the onset of Indian summer monsoon. J Clim 27:126–139